JOURNAL OF GUIDANCE, CONTROL, AND DYNAMICS
Vol. 28, No. 3, May–June 2005

Cybernetic Analysis of Perspective Flight-Path Display Dimensions

M. Mulder* and J. A. Mulder†
Delft University of Technology, 2629 Delft, The Netherlands

Perspective flight-path displays, presenting the future trajectory to be flown through a three-dimensional tunnel- or highway-in-the-sky, are likely to become the primary flight displays of future cockpits. A crucial design parameter is the size of the virtual tunnel as it determines the tradeoff between pilot path-following performance and workload. An information-theoretical and control-theoretical analysis is presented that aims at gaining an in-depth understanding of the effects of the tunnel size on pilot manual control behavior. The theoretical findings are verified in two pilot-in-the-loop experiments, one conducted in a fixed-base simulator and one in real flight. In the simulator experiment, it is shown that through pilot multiloop model identification the effects of reducing the tunnel size can be directly related to pilot/vehicle bandwidth and stability margins. The use of pilot models allows an objective quantitative analysis of the effect of the tunnel size compared to the subjective, qualitative surveys conducted in the past. The flight-test experiment supports the main findings of the simulator experiment but also reveals that pilot performance in actual flight is less consistent and also lower than measured in the flight simulator.

Nomenclature

H_t	=	tunnel height
V_{tas}	=	aircraft true airspeed
v_e	=	aircraft vertical position error
W_t	=	tunnel width
x_e	=	aircraft lateral position error
γ_e	=	aircraft flight-path angle error
δ_a, δ_e	=	aileron, elevator control
ϕ, θ	=	aircraft roll, pitch attitude
φ_m	=	phase margin
χ_e	=	aircraft track angle error
ψ_e	=	aircraft heading angle error
ω_c	=	crossover frequency

Introduction

RESEARCH indicates that a perspective flight-path display, a contact analog display that shows the future trajectory as a virtual tunnel- or highway-in-the-sky, has important advantages over conventional displays. It allows high-precision manual trajectory following,[1–8] it improves pilot situation awareness,[9,10] and it is compatible with a variety of other control and monitoring tasks.[7,11]

In principle, the size of the tunnel (the width and height of the box) reflects the limits within which the aircraft must remain to satisfy the flight-path constraints. Guiding the aircraft through the tunnel is essentially a boundary control task, with the boundaries set by the tunnel size, and the preview of the trajectory ahead allows pilots to act in different ways.[6,7,12] A continuum exists between the strategy of continuously compensating for all guidance errors, error-correcting control, and the strategy of disregarding these errors as long as the spatial and temporal constraints are satisfied, error-neglecting control. The freedom in adopting a strategy is set by the tunnel size: Smaller tunnels require pilots to put much of their attention to the guidance task to keep the aircraft in the tunnel. Hence, the tunnel size implicitly commands the required level of path-following performance, and its functionality for this purpose has been shown in previous investigations.[2,4,6,7,13–15]

Wilckens investigated the effects of a range of tunnel sizes (20–400 m) on pilot control activity and tracking performance, in a task of following a straight trajectory.[2] Pilot control activity was found to increase for smaller tunnels. The same was found to be true for the path-following performance, but only to a certain level: Reducing the size of the tunnel "too much" led to a deterioration of performance. With use of a qualitative diagram (Fig. 1), a U-shaped relation was suggested between the tunnel size and performance. As the tunnel size increases, performance reduces as the perception of the aircraft position relative to the tunnel centerline becomes more difficult: the sensitivity contribution to tracking errors, the first boundary in Fig. 1. As the tunnel size decreases, the tracking accuracy needs to improve, requiring a more tight control. Because of the inherent human perception and action limitations, for example, time delay, the overall system gain can only increase up to a point where the stability margins become too small, resulting in a lack of damping. This leaves the second boundary in Fig. 1, the so-called stability contribution to tracking errors. Hence, an optimal tunnel size results that depends on the level of pilot proficiency with the tunnel display: For more experienced pilots the optimal tunnel size will be smaller.

Grunwald compared two tunnel sizes (91 and 137 m) in a task of flying curved approaches, for a tunnel display augmented with a flight-path predictor symbol. An improved performance and larger pilot control activity for the smaller tunnel was reported.[4] These findings were confirmed by Theunissen and Mulder,[13] who evaluated tunnel sizes of 22.5, 45 and 90 m.

The previous investigations are consistent in reporting a tradeoff between performance and pilot control activity, with the latter variable taken as a metric for workload. These findings, however, are all based solely on empirical performance-related data, obtained in fixed-base flight simulators, and most important, they were not supported by a control-theoretical analysis. A more theoretical approach could allow us to determine the acceptable upper and lower limits in the tunnel size. Although Wilckens[2] suggested a deterioration of tracking performance when decreasing the tunnel size beyond a certain level, his empirical method did not offer solid arguments to support this phenomenon, nor was it supported by experimental later studies (see Refs. 4 and 13–15). In other words, although the

Presented as Paper 2002-4929 at the AIAA Guidance, Control, and Navigation Conference, Monterey, CA, 5–8 August 2002; received 25 November 2003; revision received 3 March 2004; accepted for publication 3 March 2004.

*Assistant Professor, Control and Simulation Division, Faculty of Aerospace Engineering, Kluyverweg 1; m.mulder@lr.tudelft.nl. Member AIAA.

†Professor, Chairman of the Control and Simulation Division, Faculty of Aerospace Engineering, Kluyverweg 1; j.a.mulder@lr.tudelft.nl. Member AIAA.

investigations up until now have indicated that the first boundary in Wilckens's diagram indeed exists, in the present research we will provide experimental as well as theoretical evidence for the second boundary in Wilckens's diagram.

The investigation is limited to the basic tunnel display, that is, without display augmentation such as the flight-path predictor symbol. Presenting additional symbology changes the equivalent dynamics of the system to be controlled[4,7,8] and could shift the boundaries for stability we aim at investigating here. Because it is likely that adding symbology will help the pilot in conducting his task, the results presented in the following text may well be considered to represent a lower bound.

The purpose of this paper is twofold. First and foremost, a cybernetic control-theoretical study is presented that aims at gaining a fundamental understanding of the effects of the tunnel size on pilot manual control behavior and to investigate the validity of Wilckens's[2] second boundary. Second, the results of two experiments will be described. The first experiment, conducted in a fixed-base part-task flight simulator, was designed to validate the cybernetic pilot model.[15] The second experiment was aimed at investigating the effects of reducing the tunnel size in real flight.[16]

Results of a Control-Oriented Analysis

In control-theoretical terms, Wilckens's[2] second boundary in Fig. 1 represents the limit to tracking performance, that is, maximum bandwidth, due to the minimum requirement of closed-loop system stability, that is, minimum phase margin. The investigation that follows aims at clarifying this relationship in detail for the multiloop control task of flying an aircraft along a reference trajectory. Only the control of the aircraft lateral motions is discussed. Although the aircraft longitudinal motions are fundamentally different, the approach presented here remains the same.

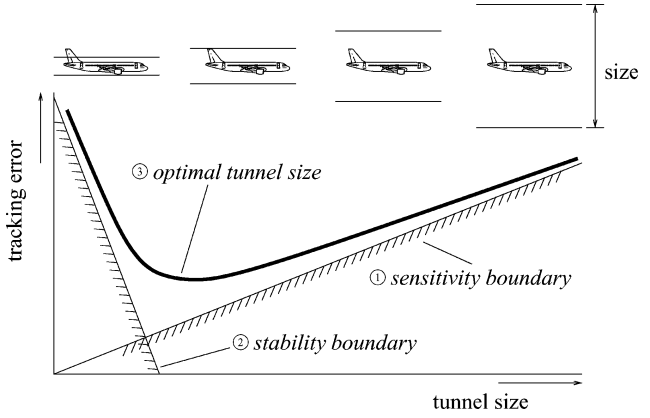

Fig. 1 Qualitative relation between tunnel size and pilot tracking error as suggested by Wilckens.[2]

Model of the Closed-Loop Pilot/Aircraft System

Figure 2 shows the closed loop system that is the starting point here. The aircraft dynamics are modeled by a linear cascaded model structure representing the three primary control variables: attitude (roll angle ϕ), flight path (track-angle error χ_e), and position (position error x_e). The error variables indicate that they are related to the reference trajectory. This structure for the lateral dynamics has been used in most of the earlier tunnel display investigations.[8,17,18] The dynamics are representative for a coordinated aircraft augmented with a turn coordinator and yawdamper, yielding a well-damped Dutch roll and reducing the lateral dynamics to the roll subsidence lag. Hence, pilots can control the aircraft through ailerons only. Also, the side slip β is small, and because the drift angle is assumed negligable, the aircraft track angle error χ_e equals the heading angle error ψ_e. The analysis that follows is representative for fast airplanes: For slower airplanes or helicopters the results are likely to be different; they are beyond the scope of this paper.

Three disturbance signals are inserted, i_1, i_2 and i_3, that represent atmospheric turbulence effects. The aircraft used in the investigation is a Cessna Citation 1, a small two-engine business jet, at a velocity V_{tas} of 70 m/s. Then, $K_\phi = 5.5$, and $\tau_\phi = 0.45$ s (Ref. 7).

Pilot control behavior is modeled as a linear serial feedback mechanism, closing the loops of attitude (the inner loop), flight path (the middle loop), and position (the outer loop), respectively, and a remnant signal n that represents all nonlinearities that cannot be described using the linear model.[19] Applying the well-known crossover model[19] yields the pilot model structure and parameters as shown in Fig. 2. In Fig. 2, the right dashed box shows the aircraft lateral dynamics $H_{\text{ac}}^{\text{in}}$, $H_{\text{ac}}^{\text{mid}}$, and $H_{\text{ac}}^{\text{out}}$, representing the roll subsidence, turn coordination, and path integration, respectively. The left dashed box shows the pilot model for the manual control of the lateral motion. A serial structure is chosen, where the pilot sequentially closes the loops of the aircraft attitude ϕ ($H_{\text{sp}}^{\text{in}}$), flight-path error χ_e ($H_{\text{sp}}^{\text{mid}}$) and position error x_e ($H_{\text{sp}}^{\text{out}}$). Here g_0 represents the gravity constant. Because of the aircraft dynamics, all pilot equalization can be put in the inner loop: A lead equalization is necessary to cancel the roll subsidence lag τ_ϕ. The aircraft turn coordination and path-integration dynamics are integrators, and the middle and outer loops are closed through a proportional gain. The pilot model parameters represent the inherent human limitations, neuromuscular dynamics (ω_n, ζ_n) and time delay τ, and the equalization, inner-loop lead τ_L^{in} and gain $K_{\text{sp}}^{\text{in}}$, middle-loop gain $K_{\text{sp}}^{\text{mid}}$, and outer-loop gain $K_{\text{sp}}^{\text{out}}$. In the analysis to follow the limitation variables are fixed: $\omega_n = 9.0$ rad/s, $\zeta_n = 0.1$, and $\tau = 0.3$ s. The remnant n is set to zero.

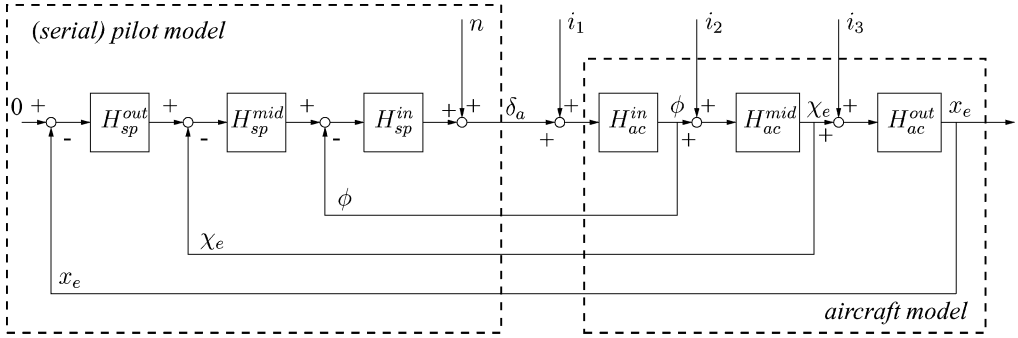

$$
\begin{aligned}
H_{sp}^{in} &= K_{sp}^{in}\,(1+\tau_L^{in}s)\left(\frac{\omega_n^2}{\omega_n^2+2\zeta_n\omega_n s+s^2}\right)e^{-s\tau} \\
H_{sp}^{mid} &= K_{sp}^{mid} \\
H_{sp}^{out} &= K_{sp}^{out}
\end{aligned}
\qquad
\begin{aligned}
H_{ac}^{in} &= H_{\delta_a}^{\phi} = \frac{K_\phi}{(1+\tau_\phi s)s} \\
H_{ac}^{mid} &= H_{\phi}^{\chi_e} = \frac{g_0}{V_{tas}}\frac{1}{s} \\
H_{ac}^{out} &= H_{\chi_e}^{x_e} = V_{tas}\frac{1}{s}
\end{aligned}
$$

n is the pilot remnant signal

i_1, i_2, i_3 are disturbance signals

Fig. 2 Closed-loop, linear pilot/aircraft system.

Effects of Bandwidth and Stability on Tracking Performance

It may now be investigated how the pilot equalization parameters K_{sp}^{in}, τ_L^{in}, K_{sp}^{mid}, and K_{sp}^{out}, determine the multiloop system bandwidth (expressed in the crossover frequencies ω_c^{in}, ω_c^{mid}, and ω_c^{out} of the inner, middle, and outer loops, respectively) and stability margins (expressed in the phase margins φ_m^{in}, φ_m^{mid}, and φ_m^{out} of the three loops), as well as the tracking performance.

A frequency domain analysis showed that, first, the inner loops serve the outer loops: A well-stabilized, high-bandwidth for the inner-loop control (attitude) is beneficial to achieve a well-stabilized, high-bandwidth middle loop (flight path). The same holds for the middle loop serving the outer loop. When the bandwidth of a particular loop approaches the bandwidth of the loop one step lower in the hierarchy, the stability margin of that loop drops rapidly. Hence, for stability reasons the following relation holds: $\omega_c^{in} > \omega_c^{mid} > \omega_c^{out}$. (In this respect, a well-known rule of thumb is that the bandwidth of a particular loop should be approximately one-third of the bandwidth of the loop lower in the hierarchy.) An important consequence of this result is that to increase the bandwidth of a loop while maintaining a sufficient stability margin, the bandwidths of basically all loops lower in the hierarchy must increase as well. Second, the quality (in terms of bandwidth, stability) of an inner loop is more important for the quality of the loop one step higher in the hierarchy than for the loops that are two or more steps higher in the hierarchy. That is, the properties of the position feedback are affected primarily by the characteristics of the track error feedback loop and hardly by the attitude feedback properties. Third, it was found advantageous for the pilot inner-loop lead τ_L^{in} to be slightly larger than the lead necessary to cancel the aircraft roll subsidence lag τ_ϕ. In this case, ω_c^{in} can increase considerably for the same level of inner-loop stability, which is beneficial in particular for the middle loop.

The characteristics of the hierarchical control system in the frequency domain are directly related to the tracking performance. Figure 3 shows the standard deviations (STDs) of the pilot control δ_a and the aircraft attitude ϕ, flight-path error χ_e, and position error x_e, as a function of the outer-loop crossover frequency ω_c^{out}, for the 12 possible combinations of 4 inner-loop crossover frequencies ($\omega_c^{in} = 1.5$, 2.0, 2.5, and 3.0 rad/s, with $\tau_L^{in} = 0.75$ s) and 3 middle-loop crossover frequencies ($\omega_c^{mid} = 0.5$, 0.8, and 1.1 rad/s). Thus, the settings for the inner and middle loops are fixed, and Fig. 3 shows how the STDs of the main state variables change when the outer-loop bandwidth increases (black lines running from left to right). For all situations, four levels (20, 40, 60, and 80 deg) of the corresponding outer-loop phase margins φ_m^{out} are shown as well (gray lines running from top to bottom); the results for $\varphi_m^{out} < 15$ deg were discarded. Furthermore, these results were computed for the case where the pilot remnant n as well as disturbance signal i_3 are zero and where both i_1 and i_2 are defined as a sum of sinusoids, listed in Table 1.

Figure 3 shows that, first, when the inner loop crossover ω_c^{in} increases, the pilot control activity becomes larger, whereas the variations in the aircraft attitude and flight-path and position errors decrease. Vice versa, a sloppy (low-bandwidth) inner loop

Table 1 Definition of forcing function signals i_1 and i_2

	Input signal i_1			Input signal i_2		
j	k_{1_j}	ω_{1_j}, rad/s	A_{1_j}, deg	k_{2_j}	ω_{2_j}, rad/s	A_{2_j}, deg
1	4	0.3068	0.5859	5	0.3835	2.1309
2	11	0.8437	0.6160	12	0.9204	1.9710
3	17	1.3039	0.6593	18	1.3806	1.7856
4	25	1.9175	0.7299	26	1.9942	1.5364
5	31	2.3777	0.7836	32	2.4544	1.3706
6	37	2.8379	0.8312	38	2.9146	1.2276
7	47	3.6049	0.8856	49	3.7583	1.0192
8	61	4.6786	0.9009	62	4.7553	0.8412
9	82	6.2893	0.8319	83	6.3660	0.6503
10	107	8.2068	0.7109	109	8.3602	0.5048
11	149	11.4282	0.5445	151	11.5816	0.3692
12	197	15.1097	0.4218	199	15.2631	0.2819

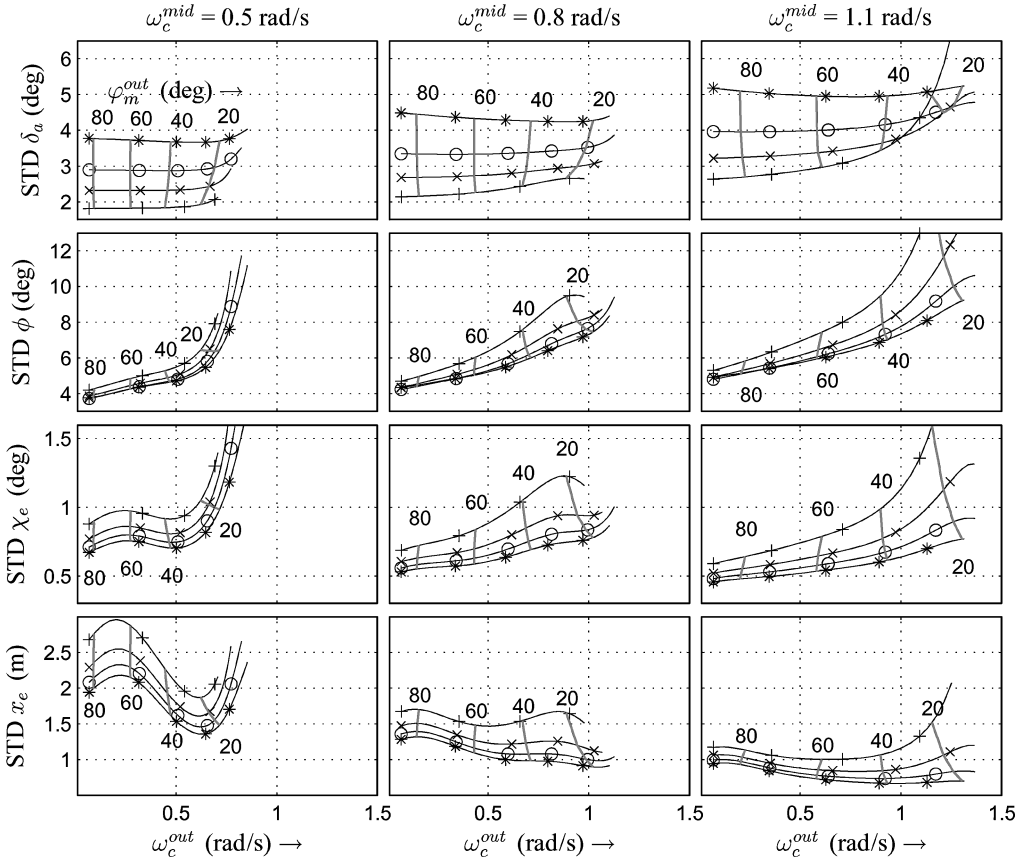

Fig. 3 Results from the control-theoretical analysis: the standard deviations of the four key variables of Fig. 2 (δ_a, ϕ, χ_e and x_e) are shown for the 12 combinations of four inner-loop crossover frequencies (+, ω_c^{in} = 1.5 rad/s; x, ω_c^{in} = 2.0 rad/s; o, ω_c^{in} = 2.5 rad/s; and *, ω_c^{in} = 3.0 rad/s) and three middle-loop crossover frequencies ω_c^{mid} (represented by the columns), as a function of the outer-loop crossover frequency ω_c^{out}.

deteriorates the performance in the outer loops. These effects are smaller for larger values of ω_c^{in}. Second, independent of the inner-loop and the outer-loop characteristics, when the middle-loop crossover ω_c^{mid} increases, pilot control activity and aircraft attitude variations become larger, while at the same time the path-following performance (flight-path and position errors) improves considerably. In particular the position error benefits from a tight, high-bandwidth feedback of flight path. Third, when the outer-loop crossover ω_c^{out} increases, but remains below ω_c^{mid}, control activity remains almost the same, attitude variations increase, and position tracking performance improves, whereas flight-path errors grow slightly. When ω_c^{out} approaches ω_c^{mid}, however, the pilot control activity and aircraft attitude variability increase, and path-following performance, both in terms of track and position errors, starts to deteriorate. These situations are also characterized by a considerable reduction of the outer-loop phase margin φ_m^{out}. Hence, the analysis indeed suggests that an optimal position error tracking performance exists: The variations in x_e are smallest when ω_c^{out} remains below ω_c^{mid} (except for the smallest value of ω_c^{mid}) and when the outer-loop phase margin is about 30–50 deg.

Conclusions from the Control-Theoretical Analysis

The model-based investigation shows that when the bandwidth of the outer-loop (position error) feedback increases, position tracking performance improves. However, when the outer-loop bandwidth approaches the bandwidth of the pilot/aircraft system that serves this loop (the combined pilot feedback of attitude and flight path), performance deteriorates because of a rapid decrease in the stability margin. Hence, from a control-theoretic point of view, the optimum in position performance, suggested by Wilckens,[2] indeed exists, with the maximum limit to performance caused by the stability requirement. In the next section, it will be described how the size of the tunnel sets the requirements for the tracking performance.

Results of an Information-Centered Analysis

It was shown earlier that, to track a trajectory, the pilot must perceive the aircraft attitude, flight path, and position and use these variables in three hierarchical feedback loops. In this section, it will be investigated how the pilot perceives these variables from the display. A perspective flight-path display is not different from a conventional artificial horizon display in that the aircraft pitch and roll attitude can be perceived from the horizon. The perception of the aircraft position and flight path relative to the tunnel is not straightforward, however, and has been the subject of a comprehensive study conducted by Mulder.[7,20,21]

Texture Gradients: Optical Splay and Optical Density

The central hypothesis in Mulder's work[7,20,21] is that the main visual stimulus when moving through the tunnel is that of an approach to a surface, with the surfaces represented by the four tunnel walls (the left and right vertical walls and the top and bottom horizontal walls) constraining the aircraft motion. Perceptual psychologists showed that approaching a surface yields an optical expansion pattern that contains essential information about the observer's motion: the texture gradients.[22,23] The projection of lines parallel to the viewing direction conveys optical splay angle information, the gradient of perspective. The projection of lines perpendicular to the viewing direction conveys optical density information, the gradient of compression. When flying through a tunnel, and approaching one or two of the four tunnel surfaces, these gradients are essential in understanding the pilot perception of the aircraft position and flight path relative to the tunnel.[7]

Mulder's[7] approach is to dissect the tunnel geometry into a number of basis entities, illustrated in Fig. 4. (All perspective displays referred to and illustrated have a vertical geometrical field of view of 40 deg, and the screen size ratio is 4:3.) In straight tunnels, the aircraft heading attitude with respect to the trajectory, ψ_e, is reflected

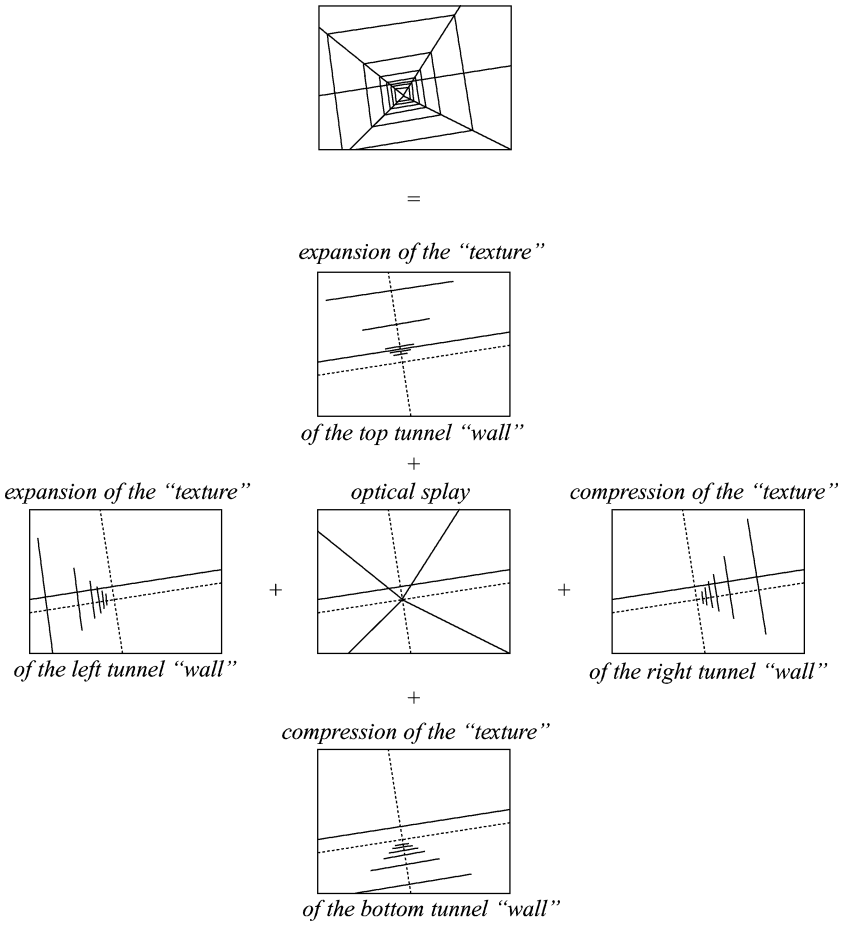

Fig. 4 Generic tunnel (top) showing a straight trajectory dissected into a number of entities that depict optical splay information (center picture) and optical density information. The dotted lines represent the horizontal pseudohorizon and the pseudovertical, crossing at the vanishing point.[7,20] The figure illustrates the situation of moving toward the right and bottom tunnel "walls."

in the position of the vanishing point, that is, the projection of the tunnel at infinity, with respect to the center of the display that represents the vehicle axis.[3] Extending the planes of the top and bottom tunnel walls to infinity yields the so-called pseudohorizon, parallel to the real horizon. The vertical difference between this pseudohorizon and the true horizon marks the slope of the trajectory. Extending the planes of the left and right tunnel walls yields a pseudovertical. The projection of the longitudinal lines connecting the tunnel frames conveys the splay angle information. The relative distribution of the vertical and horizontal frame lines with respect to the pseudovertical and pseudohorizon, respectively, conveys the density information, in a similar way as texture on the tunnel walls would. That is, when the aircraft moves to the right tunnel wall, the texture on the left tunnel wall expands and the "texture" on the right tunnel wall compresses (Fig. 4). Figure 4 shows the situation of moving toward the right and bottom tunnel walls.

Perceiving Position and Flight-Path Errors

In this section it will be shown how pilots can perceive where they are relative to the nominal trajectory (the position error) and where they are going relative to the nominal flight path (the flight-path angle error) for the case of straight tunnel trajectories. Note that the situation for curved tunnel trajectories is markedly different and is reported elsewhere.[7,21]

In Figs. 5a and 5b, the tunnel images are shown for tunnel sizes of 20 and 40 m, respectively. Figures 5a and 5b show the situation for a zero and a nonzero lateral position error ($x_e = 5$ m).

Visual Cues for a Position Error

The optical splay angles are defined as the angles between the projections of the longitudinal lines connecting the tunnel frames and the horizon. When the aircraft is not positioned in the center of the tunnel, the splay angles change according to the following equations[20]:

$$\delta\omega_1 = -\left(\frac{2W_t}{W_t^2 + H_t^2}\right)v_e - \left(\frac{2H_t}{W_t^2 + H_t^2}\right)x_e$$

$$\delta\omega_2 = -\left(\frac{2W_t}{W_t^2 + H_t^2}\right)v_e + \left(\frac{2H_t}{W_t^2 + H_t^2}\right)x_e$$

$$\delta\omega_3 = +\left(\frac{2W_t}{W_t^2 + H_t^2}\right)v_e + \left(\frac{2H_t}{W_t^2 + H_t^2}\right)x_e$$

$$\delta\omega_4 = +\left(\frac{2W_t}{W_t^2 + H_t^2}\right)v_e - \left(\frac{2H_t}{W_t^2 + H_t^2}\right)x_e$$

$$\delta\omega_5 = -\left(\frac{2}{H_t}\right)x_e \qquad (1)$$

Note that the virtual line connecting the top of the altitude poles supporting the frames yields a fifth splay angle Ω_5. The splay angles change as a function of only the aircraft position relative to the trajectory, with the lateral and vertical position errors coupled in splay. The splay angle gains [the properties between the backets in Eq. (1)] depend only on the tunnel size. Also, inasmuch as it is a line property, the splay angle is independent of the part of the line being perceived: The splay gain is constant (for straight tunnel segments).[7]

The optical density is conveyed by the displacements of the frame lines relative to the pseudohorizon and the pseudovertical. Lateral displacement changes from the pseudovertical depend on only the lateral position error x_e (Ref. 20):

$$\delta\epsilon_{i\infty} = +\kappa(1/D_i)x_e, \qquad \delta\eta_{i\infty} = -\kappa(1/D_i)x_e \qquad (2)$$

with κ a scaling factor that depends on the field of view of the perspective projection and the screen size and D_i the distance ahead to the frame i involved. Similarly, the changes in the vertical displacements relative to the pseudohorizon ($\delta\mu_{i\infty}$ and $\delta\nu_{i\infty}$) are a function only of the vertical position error v_e. The density gain [$1/D_i$ in Eq. (2)] depends on the distance to the frame elements involved, and because of the forward motion along the tunnel, the density gains are not constant.

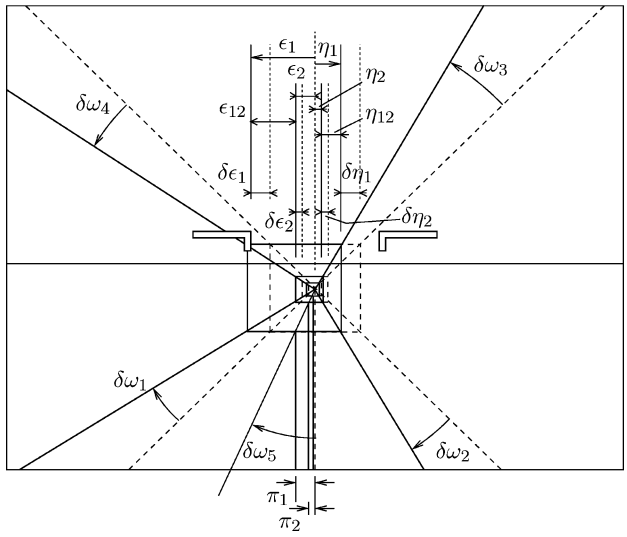

a) $W_t = H_t = 20$ m

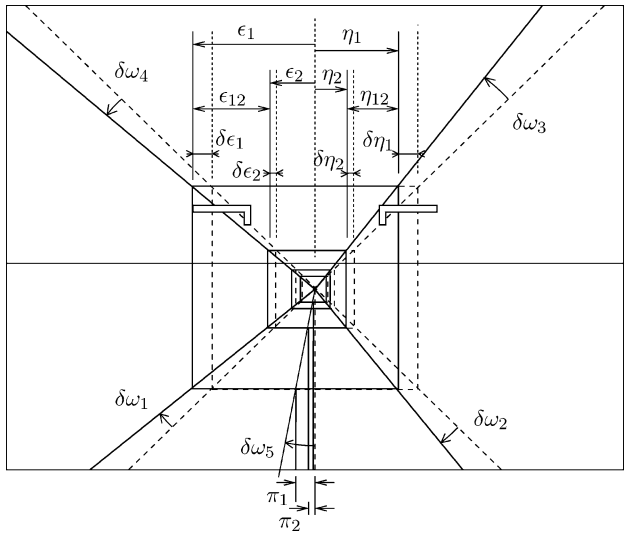

b) $W_t = H_t = 40$ m

Fig. 5 Visual cues for a lateral position error x_e in a straight tunnel. The dashed and continuous lines show the tunnel image for a zero and a nonzero (+5 m) lateral position error, respectively. The heading angle error ψ_e is zero.

Visual Cues for a Flight-Path Angle Error

Flight path information is conveyed through the change of the tunnel perspective. Here, the derivatives of optical splay, the splay angle rates, and optical density, the density rates, are the main optical sources of information for perceiving the aircraft motion relative to the trajectory. The splay angle rates are a function of the flight-path angle error in both the lateral and the vertical direction, for example, for splay angle rate $\dot{\omega}_1$ one obtains

$$\dot{\omega}_1 = -\left(\frac{2W_t}{W_t^2 + H_t^2}\right)V_{\text{tas}}\gamma_e - \left(\frac{2H_t}{W_t^2 + H_t^2}\right)V_{\text{tas}}\chi_e \qquad (3)$$

with V_{tas} the aircraft velocity and γ_e and χ_e the vertical and lateral flight-path angle errors, respectively. The splay angle rate gains are identical to the splay angle gains.

The density rates depict flight-path information in an uncoupled fashion: The vertical density rates convey the vertical flight path error γ_e, etc. When flying through the tunnel, the frames move toward

the observer, and a change in the relative displacements between the frames could be difficult to perceive.[20]

Finally, when considering straight tunnels, the tunnel display's vanishing point conveys the aircraft heading angle with respect to the trajectory, ψ_e, a property that does not depend on the size of the tunnel. When the effects of side slip and wind are negligable, χ_e is approximately equal to ψ_e, and so in this case χ_e can be perceived through the vanishing point.

Effects of the Tunnel Size

The tunnel size affects primarily the display of the aircraft position error relative to the trajectory. Smaller tunnels allow pilots to have a better estimate of the center of the tunnel frames and, therefore, of the location of the nominal trajectory. A comparison of Figs. 5a and 5b illustrates that for smaller tunnels the changes in the projection of the tunnel geometry on the screen caused by a position error are much more salient.

First, the optical splay angle gains depend only on the tunnel size. Substituting $H_t = W_t$ and $v_e = 0$ in Eq. (1), one obtains for the splay angle changes due to a lateral position error x_e

$$\delta\omega_1 = \delta\omega_4 = -x_e/W_t, \qquad \delta\omega_2 = \delta\omega_3 = +x_e/W_t \tag{4}$$

Hence, the tunnel size acts as a scaling factor, a gain for the change in splay caused by a position error. This scaling effect was first shown by Wilckens[2] and led Theunissen to allocate the term error gain to the tunnel size.[14]

The frame displacements are independent of the tunnel size, an effect that can be seen when comparing in Figs. 5a and 5b the values of these cues, for example, $\delta\epsilon_1$ or $\delta\eta_1$. They do appear, however, much larger in relation to the size of the frames themselves. Also, for larger tunnels, the displacements of the altitude poles (π_i in Fig. 5) remain the same as for smaller tunnels, which could be a useful property of these poles.

The presentation of flight-path angle error through the tunnel motion perspective and the vanishing point is marginally affected by the tunnel size. The splay angle rates are scaled by the tunnel size and the velocity [Eq. (3)]. For smaller tunnels, the effect of a nonzero flight path will be larger and results in a sweeping motion of the longitudinal lines connecting the tunnel frames.

Finally, the tunnel size affects the perception of velocity. The human perception of speed is known to be determined by two effects: optical edge rate and global optical flow rate.[24] The optical edge rate is defined as the velocity with which local discontinuities (such as the frame lines perpendicular to the forward motion) cross a part of the observer's field of view. The global optical flow rate is defined as the quotient of the forward velocity and the distance to the plane the observer moves parallel with. In our case, the optical edge rate is reflected in the speed at which the tunnel frames pass the observer: It is independent of the tunnel size. The global optical flow rate equals $V_{\text{tas}}/(W_t/2)$: Decreasing the tunnel size brings the tunnel surfaces (the walls) with respect to which one is moving closer to the observer, resulting in a larger global optical flow rate and, therefore, a higher subjective velocity. In conclusion, for smaller tunnels it is as if the aircraft velocity is higher than in larger tunnels. This effect can also be explained using Fig. 5: For the smaller tunnel it appears as if the first frame is located farther away. However, it is not, so when approaching the frame it seems to move faster toward the observer than in the larger tunnel.

Conclusions from the Information-Centered Analysis

The optical concomitants of approaching the tunnel walls, the texture gradients of splay and density, allow pilots to perceive directly their position and motion relative to the reference trajectory.[7,20] The tunnel size affects primarily the perception of the position error, and to a lesser extent, the flight-path error, by scaling the amplitude with which they are presented by the display. The information analysis provides clear evidence for the sensitivity boundary of Wilckens:[2] When the tunnel size increases, the effect of a position error on the changing tunnel perspective becomes smaller. For very large tunnels pilots will not be able to see small position errors from the display because the projection of the tunnel geometry on the display hardly changes.

For very small tunnels, the projection of the tunnel geometry will rapidly sweep across the screen. As an example, when reducing the tunnel height H_t to, for instance, 1 m, the tunnel frames will only be central on the screen when the vertical position error is almost zero. In all other cases, the aircraft will be flying below or above the virtual plane depicted by the extremely flattened tunnel. In this case, the best strategy for a pilot may well be to keep the aircraft at a certain height above this surface, accepting a nonzero vertical position error and putting more attention to the control of the vertical flight path relative to the surface. Therefore, although the relation between the tunnel size and the position control bandwidth appears straightforward (with smaller tunnels requiring a higher bandwidth), the effect on pilot behavior may not be as simple as it seems. Although pilot behavior can, in a well-defined situation, be accurately described using linear models, pilots remain essentially opportunistic, nonlinear systems, who will adapt their strategies to the situation at hand. This needs to be investigated through pilot-in-the-loop experiments.

Experiment 1: Tunnel Tracking in a Fixed-Base Flight Simulator

Experiment 1 aimed at complementing the earlier, qualitative, tunnel-size investigations with a control-theoretic approach. For this purpose, the experiment was designed in such a way that the pilot control behavior could be identified and described in a mathematical model. This allows us to investigate not only the consequences of pilot behavior (such as tracking performance and control activity) but also the internal mechanisms causing this behavior to happen.

The identification of pilot control behavior in the closed-loop tunnel tracking task is a tedious procedure, and a number of simplifying assumptions had to be made to make it feasible.[7] First, the linear aircraft dynamics of Fig. 2 were used to simulate the aircraft motions. Second, the atmospheric turbulence is modeled through the insertion of two independent forcing functions, i_1 and i_2 in Fig. 2 (i_3 is not used). Third, only the lateral motion in the tunnel was investigated.

Method

Apparatus

The experiment was done in a fixed-base, part-task flight simulator. Subjects were seated in front of a 17 in. color monitor, the eye distance to the screen was approximately 0.80 m. They controlled an electrohydraulic side-stick with two degrees of freedom: aileron and elevator (not used). The lateral side-stick dynamics represented a linear mass–spring–damper system with bandwidth 16.3 rad/s and damping 0.53 (Ref. 7).

Subjects and Instructions to Subjects

Three professional pilots and one student pilot participated in the experiment (Table 2). They were instructed to control the aircraft lateral motion through the tunnel as accurately as possible, that is, the position error must be minimized.

Table 2 Characteristics of the pilot subjects in experiments 1 and 2

Pilot	Sex	Age	Hours	Types of aircraft
			Experiment 1	
A	M	30	1600	Single-engine, Cessna Citation II, Fokker 100, B767
B	M	33	4000	Single-engine, B767, MD-11
C	M	30	1600	Single-engine, Cessna Citation II, Fokker 100, B767
D	M	29	50	Cessna Citation I (flight simulator)
			Experiment 2	
A	M	62	12900	Single-engine, DC-3, DC-8, B747, Cessna Citation II
B	M	34	1200	Single-engine, Cessna Citation II

Independent Variables

Two independent variables were varied in the experiment: 1) the tunnel size W_t (four levels): 80, 40, 20, and 10 m; and 2) the velocity V_{tas} (three levels): 50, 70, and 100 m/s. Note that the aircraft velocity affects its handling characteristics: For larger velocities, the roll subsidence lag τ_ϕ decreases, reducing the need for pilot inner-loop lead equalization, making the control easier.[7,19]

Experimental Design and Procedure

A full-factorial within-subjects design was applied, yielding 12 conditions. The conditions were randomized over the experiment. Each subject conducted three training sessions (36 runs) before completing 5 replications of all experimental conditions (60 runs) that served as the measurements. A single run lasted 101.92 s, consisting of a run-in time of 20.0 s and a measurement time T_m of 81.92 s. When the experiment was finished, subjects were asked to complete a pilot questionnaire, including also the McDonnel subjective workload rating scale.[25] The questionnaire invited pilots to explain their control strategy and to comment on the experiment.

Tunnel Display Geometry

A generic tunnel was used (Fig. 4), with square frames ($H_t = W_t$). The reference trajectory was straight and had a downslope of 3 deg. The distance between frames was fixed at 350 m. To study the pilot behavior with the basic tunnel display geometry only, no display augmentation symbology such as the flight-path vector was presented.

Aircraft Model

The lateral motions of a Cessna Citation 1 were simulated at the three velocity conditions listed earlier. The aircraft vertical motion was fixed, resulting in a constant flight path of −3 deg. The aircraft was equipped with a yaw damper and turn coordinator, reducing the lateral dynamics to the roll subsidence motion (Fig. 2). Pilots were able to control the aircraft through aileron only; no other configuration changes were necessary.

Atmospheric Disturbances

The identification method required two independent forcing function signals to be inserted in the loop (i_1 and i_2 in Fig. 2). These signals consisted of a sum of 12 sinusoids (Table 1) and were representative for a standard turbulence.[7] The disturbance signal i_3 (representing side-slip effects) was zero: $\chi_e = \psi_e$. To allow a comparison between the aircraft velocity conditions, the disturbance signal spectra were compensated for the aircraft model characteristics.

Dependent Measures

Three types of performance variables acted as dependent measures: 1) pilot control activity, that is, aileron δ_a and aileron rate $\dot{\delta}_a$; 2) aircraft attitude variations, that is, roll angle ϕ and roll rate $\dot{\phi}$, and 3) path-following accuracy, that is, track-angle error χ_e and lateral position error x_e. The STDs of these variables represent the experimental results in the time domain. The frequency-domain data that result from the pilot model identification procedure are discussed separately.

Experiment Hypotheses

It was hypothesized that reducing the tunnel size leads to an increasing control activity, higher attitude variability, an improved path-following performance, and higher workload. Concerning the effects of the velocity, it was hypothesized that, first, because the roll subsidence lag τ_ϕ is smaller for higher velocities, pilots need to generate less lead in the inner loop, making the aircraft control easier, reducing control activity and workload in these conditions. Second, because for higher velocities the same track angle error implies larger position error rates, it was hypothesized that control of track becomes more important in these conditions.

Table 3 Results of full-factorial ANOVA on dependent measures of experiment 1[a]

	Control activity		Inner-loop measures		Path-following performance	
Variable	$\dot{\delta}_a$	δ_a	$\dot{\phi}$	ϕ	χ_e	x_e
Main effects						
V	⋆⋆	⋆⋆	•	•	⋆⋆	•
W	⋆⋆	⋆⋆	⋆⋆	⋆⋆	•	⋆⋆
Two-way interaction						
$V \times W$	•	⋆	⋆	•	⋆⋆	⋆

[a]⋆⋆, Chance level $p \leq 0.01$; ⋆, chance level $0.01 < p \leq 0.05$; o, chance level $0.05 < p \leq 0.10$ (no occurrences in this table); •, not significant. V and W stand for the velocity and tunnel size, the independent variables.

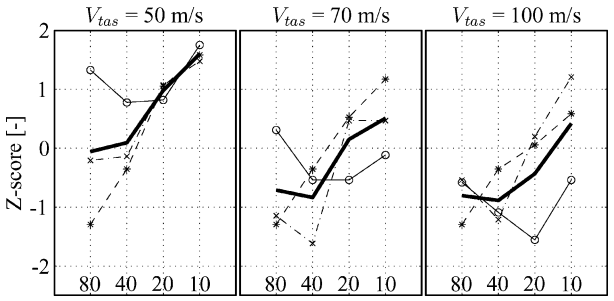

Fig. 6 Normalized effort ratings (Z-scores[7]): thick line, average over the three professional pilots and symbols, data for each individual subject.

Results

Pilot Questionnaire and Workload Ratings

Pilot comments correspond well with the information analysis: For large tunnels, pilots used the relative lateral tunnel frame displacements, in particular, the altitude poles (π_i in Fig. 5), whereas for smaller tunnels the splay angles were the primary cue for perceiving the position error.

The workload ratings (Fig. 6) show a clear increase in workload for decreasing tunnel sizes, especially for the smallest tunnels. In Fig. 6 and subsequently, the data are shown for velocity conditions 50, 70, and 100 and channel widths 80, 40, 20, and 10 m. When the velocity increases, workload reduces, an effect that is caused by the improvement in the aircraft handling (the smaller roll subsidence lag τ_ϕ).

Statistical Analysis of the Dependent Measures

The means and the 95% confidence limits of all dependent measures are shown in Fig. 7, and Table 3 shows the results of an analysis of variance (ANOVA).

Independent of the aircraft velocity, a reduction in tunnel size yielded a better position tracking performance (x_e; $F_{3,9} = 14.467$, $p < 0.01$), a larger pilot control activity (δ_a; $F_{3,9} = 17.871$, $p < 0.01$, and $\dot{\delta}_a$; $F_{3,9} = 12.612$, $p < 0.01$), and increased attitude variations (ϕ; $F_{3,9} = 34.846$, $p < 0.01$, and $\dot{\phi}$; $F_{3,9} = 23.189$, $p < 0.01$). The track angle error χ_e did not change with the tunnel size but reduced significantly for higher velocities ($F_{2,6} = 48.949$, $p < 0.01$). Furthermore, pilot control activity decreased for larger velocities (δ_a; $F_{2,6} = 121.251$, $p < 0.01$ and $\dot{\delta}_a$; $F_{2,6} = 106.443$, $p < 0.01$).

The magnitudes of the experimental STDs in Fig. 7 (for $V_{\text{tas}} = 70$ m/s) correspond fairly well with those found in the control-theoretical analysis (Fig. 3). In general, they are lower, which is because in the theoretical analysis the pilot remnant n was assumed to be zero, whereas in the experiment the remnant is, obviously, nonzero.

Pilot Model Identification

The identification of the pilot model allows the bandwidths and stability margins of the three hierarchical feedback loops (attitude, flight path, and position) to be determined, resulting in Fig. 8.

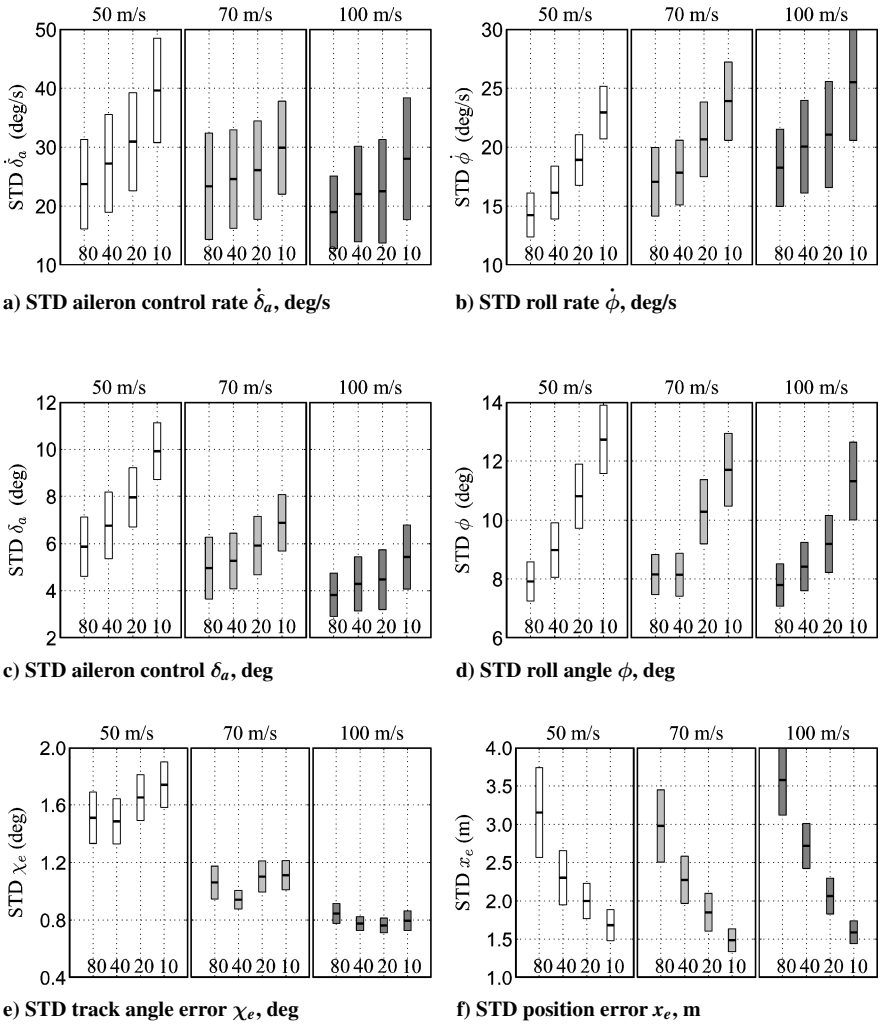

a) STD aileron control rate $\dot{\delta}_a$, deg/s **b) STD roll rate $\dot{\phi}$, deg/s**

c) STD aileron control δ_a, deg **d) STD roll angle ϕ, deg**

e) STD track angle error χ_e, deg **f) STD position error x_e, m**

Fig. 7 Means and the 95% confidence limits of the main dependent measures of experiment 1 (all subjects).

Figure 8 clearly shows that, for all velocities, the aircraft control in smaller tunnels requires a marginal increase of ω_c^{in}, a substantial increase of ω_c^{mid}, and a strong increase of ω_c^{out}. The inner-loop phase margin remains fairly constant, φ_m^{mid} reduces somewhat, and the outer loop phase margin deteriorates rapidly for the smallest tunnel. The control-theoretical analysis indicated that this can be explained by the fact that whereas ω_c^{mid} remains well below ω_c^{in}, ω_c^{out} approaches ω_c^{mid} for the smallest tunnels, which reduces the outer-loop stability margin considerably.

As far as the aircraft velocity is concerned, only the inner-loop bandwidth increases for higher velocities. This is because a faster aircraft roll response (a lower τ_ϕ) allows pilots to keep a tighter inner loop. This explains the lower workload ratings for these conditions as well.

Discussion and Conclusions

The experimental results support the predictions of the cybernetic analysis: When the tunnel becomes smaller, the bandwidths of the hierarchical pilot control system must increase to satisfy the greater demand for tracking accuracy. Previous investigations are confirmed, and also some novel insights are gained. First, although track angle error variations (STD χ_e) do not change when the tunnel size decreases, the pilot track feedback bandwidth becomes significantly larger. This shows that pilots aim at minimizing position error and illustrates that track control serves position control. It also implies that no error-neglecting control strategy is adopted. When this would have been the case, track-angle performance would have increased for smaller tunnels because then the time remaining before leaving the tunnel would remain the same.

Second, no minimum in position error performance could be found. Although the trend in the performance data suggests that the position error would further reduce when the tunnel size would be even smaller, the identified pilot models show clearly that the closed-loop stability margins decrease significantly, in particular in the outer loop (position control). When these stability margins become too small, the pilot would be forced to either hold on to a maximum outer-loop crossover (and thus a certain minimum stability margin), or to change the control strategy as a whole, for example, to one in which flight path would be the primary objective for control, resulting in a flight parallel to the nominal trajectory. In either case, position error performance would reveal a saturated control system, resulting in a minimum level of tracking performance.

Concluding, the experiment yields quantitative evidence, in the frequency domain, for Wilckens's[2] claim that there exists a boundary to tracking performance caused by the need for stability.

Experiment 2: Tunnel Tracking in Real Flight

As already stated, all previous investigations regarding the tunnel size have been conducted in part-task, fixed-base flight simulators. Experiment 2 was another attempt to complement these studies, now through investigating the effects of the tunnel size in real flight, in support of the predictions from the cybernetic analysis of experiment 1. The flight tests, conducted in May 2001, included two experiments and three demonstration flights.[16] Only the results of the experiment addressing the effects of the tunnel size will be described.

Method

Apparatus: Aircraft and Tunnel-in-the-Sky Display

The Cessna Citation 2 laboratory aircraft of Delft Aerospace, a small two-engine business jet, was used in the flight tests. To allow a comparison of the pilot behavior with experiment 1, a very

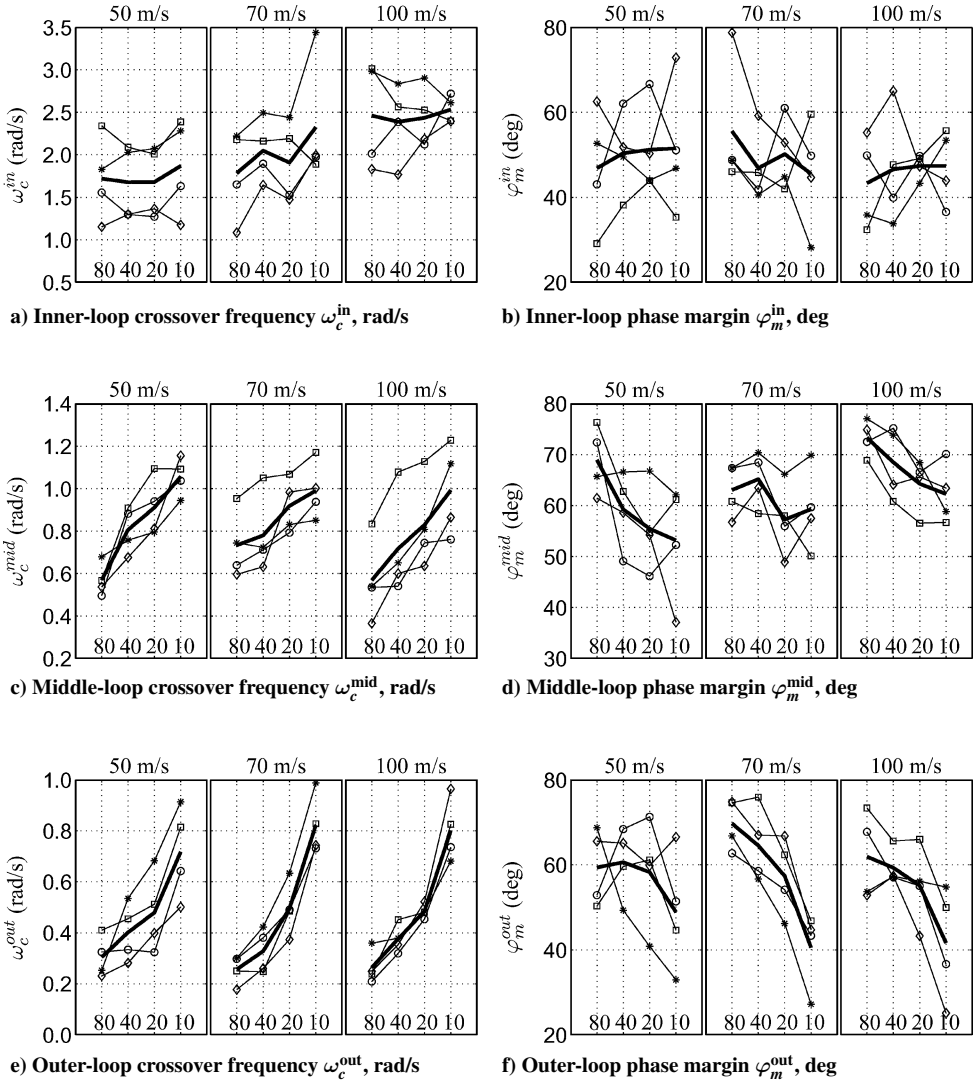

a) Inner-loop crossover frequency ω_c^{in}, rad/s **b) Inner-loop phase margin φ_m^{in}, deg**

c) Middle-loop crossover frequency ω_c^{mid}, rad/s **d) Middle-loop phase margin φ_m^{mid}, deg**

e) Outer-loop crossover frequency ω_c^{out}, rad/s **f) Outer-loop phase margin φ_m^{out}, deg**

Fig. 8 Crossover frequencies and phase margins (all subjects) computed using identified pilot model of Fig. 2: thick line, average over all subjects and symbols, data for each individual subject.

elementary tunnel display was employed: Except for the basic tunnel geometry, no additional symbology (such as a flight-path vector symbol) was presented. The display further included the conventional indicators for airspeed, altitude, and vertical speed. All information was presented on a 15-in. LCD screen that was mounted in front of the copilot's seat. The aircraft was equipped with a very accurate, hybrid, navigation system, developed in-house, using satellite positioning data smoothed by an inertial navigation system.[26]

Procedure

The two approach trajectories that were flown are shown in Fig. 9. Both trajectories start at the nondirectional beacon ROT located to the southeast of Rotterdam Airport runway 24, where the trajectories end. The first trajectory, t1, started at ROT at an altitude of 1950 ft. This altitude was maintained until after the instrument landing system (ILS) localizer was intercepted. Then the ILS glide slope was followed on final approach. The second trajectory, t2, started at ROT at an altitude of 3600 ft. Shortly after the interception of the horizontal tunnel trajectory at ROT, the trajectory downslope increased to 3 deg. Also this trajectory exactly matched the ILS glide slope on final approach.

Subjects and Instructions to Subjects

Two pilots collaborated in the experiment (Table 2). Both pilots have many flying hours on the Cessna Citation 2 laboratory aircraft. They were briefed about the goals of the flight tests and their tasks during flight. On all approaches, one pilot was the test pilot who had to intercept the tunnel, fly through it as accurately as possible, keep the airspeed constant at 150 kn (indicated airspeed), and hand over the controls to the second pilot at approximately 200 ft above ground level. The second pilot then conducted the go-around maneuver and made a shallow turn to the ROT beacon, where the next trial started. During this maneuver the test pilot had ample time to complete their workload measurement. No configuration changes were necessary: All approaches were flown with 5-deg flaps and the landing gear extended. After finishing of the flight-test program, both pilots were asked to complete an extensive pilot questionnaire. The questionnaire invited pilots to explain their control strategy and give their opinion about the apparatus, their task, and the level of situation awareness.

Visibility, Wind, and Weather Effects

The weather was fine, with a good visibility and a clear sky. During two of the four days of experimenting, however, there was a strong wind (25–35 kn, heading from the west; Fig. 9) and considerable turbulence, affecting both the roll and the yaw motions of the aircraft, resulting in considerable difficulty in flying the tunnel accurately in some trials.

Data Analysis Procedure

The time recordings (sampled at 100 Hz) could be linked exactly to certain parts of the trajectory, which allowed a comparison between, for instance, pilot performance in following the curved parts of the trajectory vs performance at final approach.[16] A total

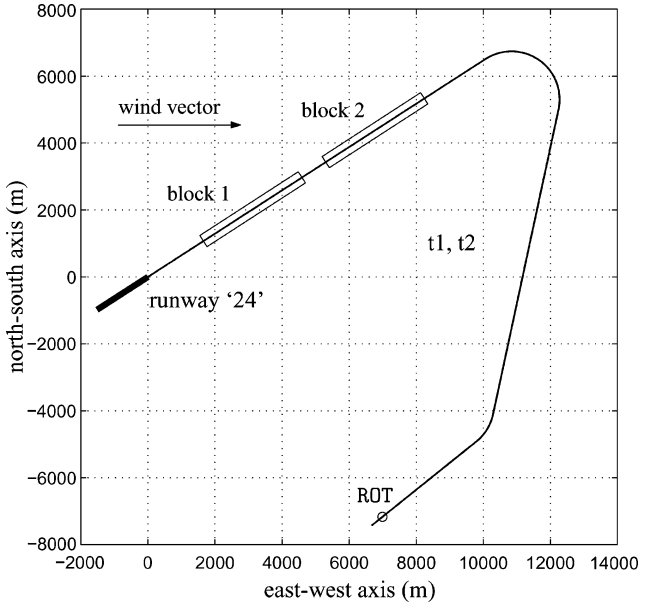

a) Horizontal plane

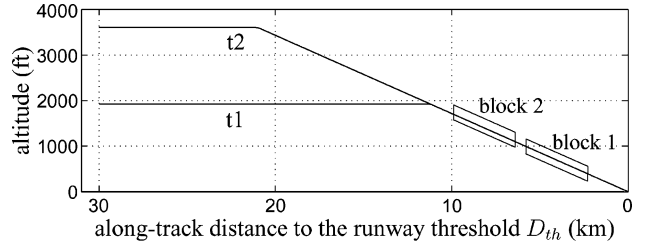

b) Vertical plane

Fig. 9 Tracks, t1 and t2 flown in experiment 2 and positions of two blocks for which data are analyzed.

of nine parts of the trajectory were selected, labeled blocks. Here only the data for the two blocks on the final approach are analyzed: blocks 1 and 2 in Fig. 9, as they represent the part of the trajectory where the aircraft is descending stationary along a straight tunnel segment, facilitating the comparison with experiment 1. With a velocity of approximately 150 kn, the along-track length of each block (3750 m) corresponds with about 50-s flying time.

Independent Variables and Experimental Design

The independent variable in the experiment was the tunnel size. Three sizes were used: 20, 40, and 80 m. Each tunnel size was repeated seven times, the last five trials served as the measurements.

Dependent Measures

The pilot tracking performance was expressed in terms of the position errors (lateral x_e and vertical v_e) as well as the flight-path angle errors (horizontal track-angle error χ_e and vertical angle-of-climb error γ_e). The pilot control activity was expressed in the variation in deflections of aileron δ_a, elevator δ_e, rudder δ_r and thrust. (Variations in engine revolutions per minute n_1 were used for this purpose.) Pilot workload was obtained using the NASA Task Load Index (TLX), a subjective workload scale.[27] The aircraft-related variables that were measured were the attitude angles ϕ and θ, the attitude rates $\dot{\theta}$ and $\dot{\phi}$, and the accelerations perpendicular to the trajectory, $\ddot{x}_e$ and $\ddot{v}_e$. Finally, the number of times the roll rate $\dot{\phi}$ exceeded a certain limit ($3 < \dot{\phi} < 5$, $5 < \dot{\phi} < 7$, and $\dot{\phi} > 7$ deg/s) was counted to study the aggressiveness of the maneuver in the lateral plane. Similarly, in the vertical plane, it was counted how often the normal acceleration n_z exceeded certain values [$1.05 < n_z < 1.15$ ($\triangle n_{z_1}$), $1.15 < n_z < 1.35$ ($\triangle n_{z_2}$), and $n_z > 1.35$ "g" ($\triangle n_{z_3}$)].

Experiment Hypotheses

The hypotheses are straightforward: Smaller tunnels result in a better path-following performance, higher control activity, higher workload, and more aggressive maneuvering.

As compared to experiment 1, the tracking task is more difficult: flying a real aircraft along the tunnel, through atmospheric wind and turbulence, controlling not only the lateral motion but also the vertical motion and the velocity as well. Hence, a worse tracking performance is hypothesized. Furthermore, in real flight pilots much better experience the effects of controlling the aircraft along the tunnel trajectory as compared to the fixed-base simulator environment, where peripheral vision cues and in particular the motion cues were absent. Hence, although the maneuvering is hypothesized to increase for smaller tunnels, resulting in more attitude variability and higher accelerations, the effects are expected to be less strong than in experiment 1. On the other hand, because of the increasing task difficulty and the greater emphasis on keeping the aircraft maneuvering within certain boundaries, the chances of finding the limits in tracking performance when reducing the tunnel size, as hypothesized by Wilckens,[2] are expected to be higher than in experiment 1.

Results

Pilot Questionnaire and Workload Ratings

The comments were very similar for both pilots. The tunnel size contributed most to the workload, followed by the strong winds during some of the flights. When asked to compare their workload with conventional ILS approaches, both pilots rated the approach with the 80-m tunnel about equal in workload, higher with the 40-m tunnel, and much higher with the 20-m tunnel. Pilots suggested to shape the tunnel more like a funnel, that is, reducing the size of the tunnel when approaching the runway in a similar way as the ILS geometry, which demands an increased tracking performance when approaching the runway threshold. Finally, both pilots commented on an excellent situation awareness, much improved as compared to the situation with conventional instruments and integrated guidance systems such as the flight director.

Both pilots rate the task of flying through smaller tunnels to be of higher workload (Fig. 10). A closer analysis of the TLX rating weightings revealed that in particular the physical load, the effort, and the performance level increased considerably for smaller tunnels, especially for the tunnel size of 20 m, indicating that smaller tunnels indeed put a much higher strain on pilots.

Time Spent Out of Tunnel

Figure 11 shows the time histories of typical approaches of both pilots for the three tunnel widths. It illustrates that the differences in tracking performance between the two pilots were quite large. Pilot A, the retired B747 captain, had considerable difficulty staying within the tunnel, even when on final approach. To quantify the time spent outside of the tunnel boundaries, three additional

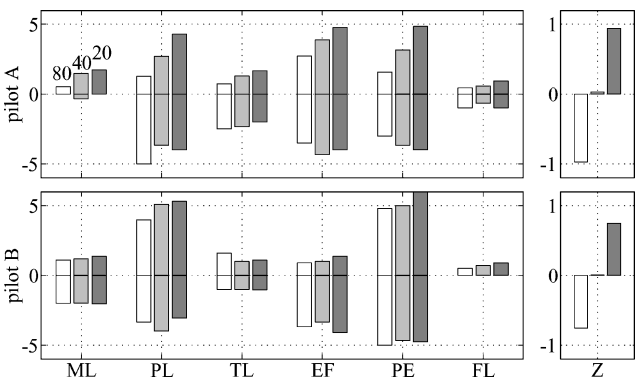

Fig. 10 NASA-TLX subjective workload scale for pilots A and B and final, normalized Z scores for 20-, 40-, and 80-m tunnel widths: averaged TLX workload ratings (positive bars) and weightings (negative bars) (left) for mental load, physical load, temporal load, effort, performance, and frustration level subscales.[27]

performance metrics were defined: the percentage of time spent out of the tunnel in the lateral dimension (but not vertical), P_{lat}, in the vertical dimension (but not lateral), P_{vert}, and in both the lateral and the vertical dimension, P_{tot}. Table 4 shows that pilot A indeed had more difficulty staying within the tunnel than pilot B, in particular in the lateral dimension. When the tunnels become smaller, the time spent out of the tunnel increases considerably, especially for pilot A. Pilot B had less difficulty keeping the aircraft in the tunnel and only sporadically spent time out of it.

Statistical Analysis of Dependent Measures

A full-factorial within-subjects ANOVA was conducted with the three tunnel widths and the two blocks as independent variables.

Table 4 Means and medians (between brackets) of the percentages of time pilot out of tunnel

	Block 1			Block 2		
Pilot	20 m	40 m	80 m	20 m	40 m	80 m
	P_{lat}, *percentage of time out-of-tunnel, lateral*					
A	38(34)	17(19)	·(·)[a]	39(33)	28(29)	11(·)
B	7(7)	·(·)	·(·)	14(16)	2(·)	·(·)
	P_{vrt}, *percentage of time out-of-tunnel, vertical*					
A	3(·)	1(·)	·(·)	12(13)	·(·)	1(·)
B	1(·)	·(·)	·(·)	·(2)	·(·)	·(·)
	P_{tot}, *percentage of time out-of-tunnel, total*					
A	13(11)	14(·)	·(·)	10(12)	·(·)	1(·)
B	·(·)	·(·)	·(·)	·(·)	·(·)	·(·)

[a]Zero percentage.

This analysis showed that the data did not differ significantly between blocks, allowing this variable to be discarded. From this it can be concluded that although block 1 is closer to the runway threshold than block 2, which would in a conventional ILS approach (with its characteristic funneling) require more emphasis on tracking performance, performance was not significantly different with the tunnel display. This illustrates one of the fundamental differences between conventional ILS approaches and tunnel display approaches.

A second ANOVA was conducted (independent variables of tunnel width W, a fixed factor with three levels, and with pilot P, a random factor with two levels) (Table 5). The means and the 95% confidence limits of the dependent measures are shown in Fig. 12. An important result from the ANOVA is that no interactions are found between pilot and width, indicating that the trends in the data due to manipulating the latter are not significantly different for both pilots.

Figure 12 shows that, for both pilots, path-following performance in terms of position errors increased significantly (x_e; $F_{2,2} = 10.515$, $p = 0.087$ and v_e; $F_{2,2} = 92.787$, $p = 0.011$) for smaller tunnels. Like the simulator experiment, no effects were found on the flight-path angle errors χ_e and γ_e. Generally, pilot control activity increases (δ_a; $F_{2,2} = 10.945$, $p = 0.084$; δ_e; $F_{2,2} = 13.021$, $p = 0.071$; and δ_r; not significant), effects of marginal statistical significance, as well as the aircraft attitude variations (ϕ; $F_{2,2} = 21.369$, $p = 0.045$, $\dot{\phi}$; $F_{2,2} = 21.816$, $p = 0.044$; and θ and $\dot{\theta}$; not significant). Furthermore, the lateral and vertical accelerations perpendicular to the track ($\ddot{x}_e$; $F_{2,2} = 41.288$, $p = 0.024$ and $\ddot{v}_e$; not significant), the roll rate counters ($\dot{\phi}_{3-5}$; $F_{2,2} = 39.514$, $p = 0.025$; $\dot{\phi}_{5-7}$; $F_{2,2} = 54.348$, $p = 0.018$; and $\dot{\phi}_{>7}$; not significant) and the g-level counters ($\triangle n_{z_1}$; $F_{2,2} = 19.601$, $p = 0.049$ and $\triangle n_{z_2}$ and $\triangle n_{z_1}$; not significant) all

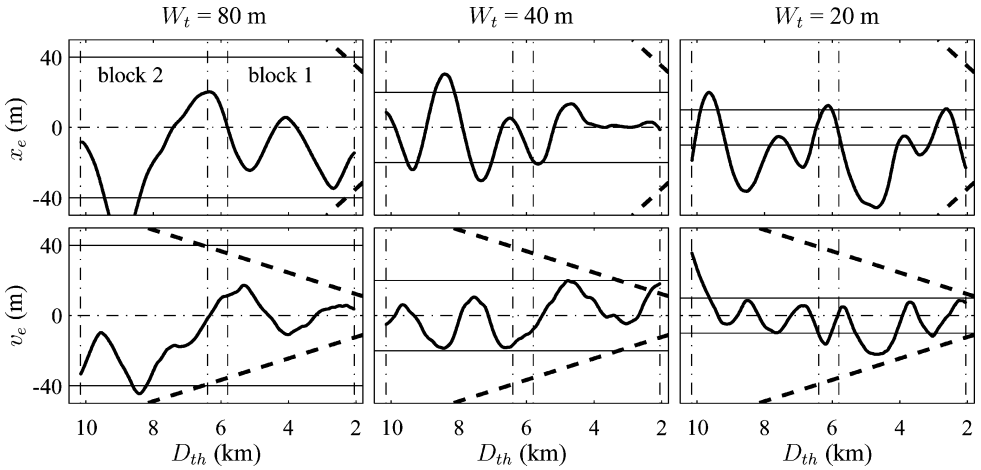

a) Three typical approaches of pilot A

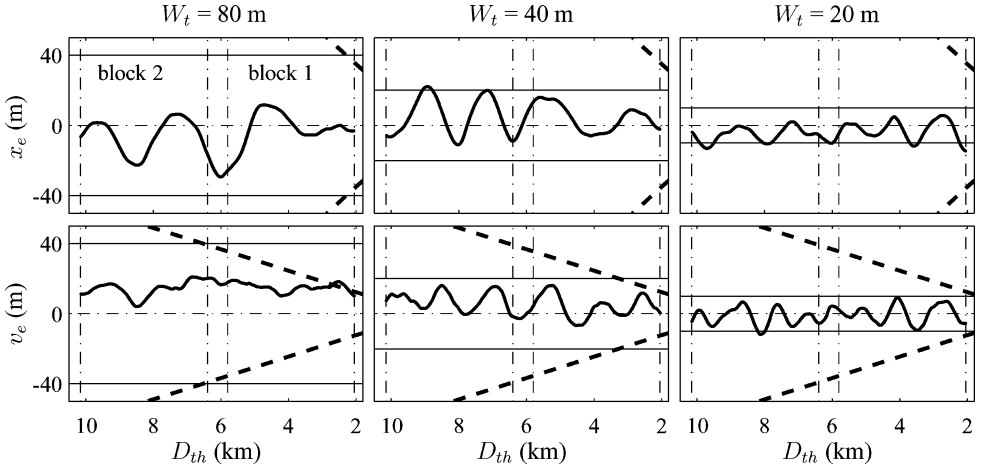

b) Three typical approaches of pilot B

Fig. 11 Lateral and vertical aircraft position relative to the nominal trajectory, as function of distance to threshold D_{th}: – – –, 1 dot deviation from ILS localizer (top, 1 dot = 1 deg error) and the glide slope (bottom, 1 dot = 0.35-deg error), typical ILS funnel geometry.

Table 5 Results of full-factorial ANOVA on dependent measures of experiment 2[a]

	Control activity		Attitude angles		Attitude rates		Flight-path angle error		Position error		Accelerations		Roll rate counters			g-level counters		
Variable	δ_a	δ_e	ϕ	θ	$\dot{\phi}$	$\dot{\theta}$	χ_e	γ_e	x_e	v_e	$\ddot{x}_e$	$\ddot{v}_e$	$\dot{\phi}_{3-5}$	$\dot{\phi}_{5-7}$	$\dot{\phi}_{>7}$	Δn_{z_1}	Δn_{z_2}	Δn_{z_3}
Main effects																		
P	•	•	⋆	•	•	•	⋆	•	⋆⋆	⋆⋆	⋆	•	•	•	○	•	•	•
W	○	○	⋆	•	⋆	•	•	•	○	⋆	⋆	•	⋆	⋆	•	⋆	•	•
Two-way interaction																		
P × W	•	•	•	•	•	•	•	•	•	•	•	•	•	•	•	•	•	•

[a]⋆⋆, Chance level $p \leq 0.01$; ⋆, chance level $0.01 < p \leq 0.05$; o, chance level $0.05 < p \leq 0.10$ (no occurrences in this table); •, not significant.

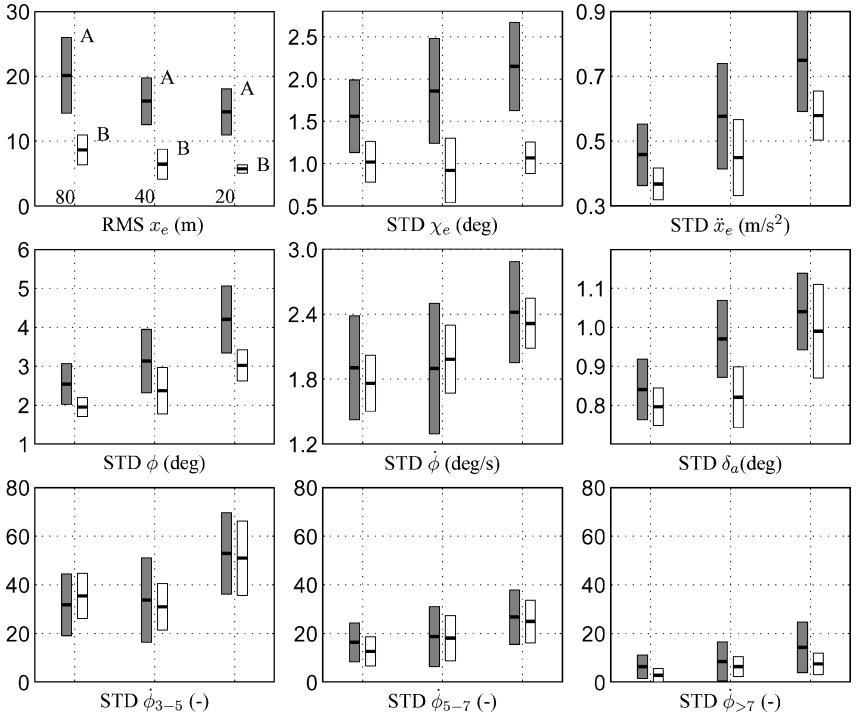

a) Performance in the lateral plane

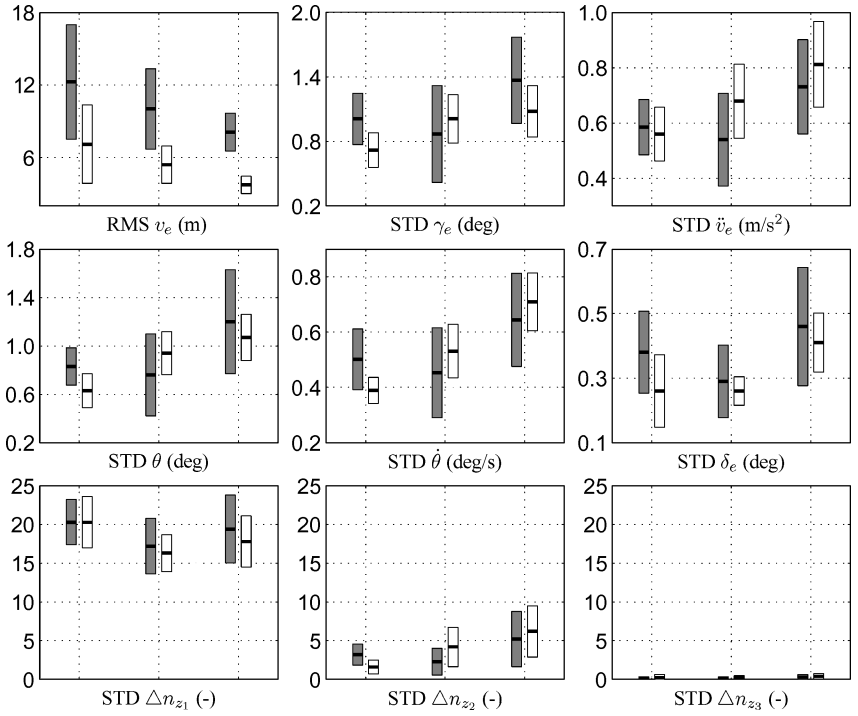

b) Performance in the vertical plane

Fig. 12 Means and the 95% confidence limits for the main dependent measures of experiment 2, as a function of the tunnel size: left, middle, and right bars are 80, 40, and 20 m, respectively, gray and white rectangles are data for pilots A and B, respectively.

increase for smaller tunnels, indicating a more aggressive aircraft maneuvering. The highest g-levels (on average, exceeding 1.15 g about 5 times per block) and roll rates (often exceeding 7 deg/s) were found for the smallest tunnels. No differences were found between pilots.

These effects are mainly caused by the smallest tunnel of 20 m: The differences between the 80- and 40-m tunnel were rather small. Also, all effects are stronger and also more clear for pilot B. Pilot B performed much better than pilot A, with even a smaller amount of control activity. Therefore, a post hoc analysis (Student Newman–Keuls, $\alpha = 0.05$) was conducted separately for both pilots. For pilot B, the effects of the tunnel size were all significant. The trends for pilot A are similar, but except for the aileron control and the roll angle variations, they were not significant.

A striking result for pilot A is that the tunnel size of 20 m was too small: The average rms x_e is almost 15 m and the mean rms v_e is almost 8 m (Fig. 12). For this tunnel size, the aircraft is out of the tunnel laterally over 40% of the time (Table 4 and Fig. 11). Hence, the performance required by the smallest tunnel was too high for the most experienced pilot, even on the stationary, final part of the approach where the effects of wind could be compensated for best.

Discussion and Conclusions

The flight tests were the first to investigate the effects of the tunnel size on pilot behavior in a real flight. The results are well in line with previous work conducted in flight simulators: Smaller tunnels yield a better performance but also result in more control effort, higher workload, and a more aggressive maneuvering. Two conclusions can be drawn from the flight tests:

First, path-following performance was found to be more variable and also considerably worse (a factor two to three) than the performance in experiment 1. Obviously, this is because the pilot task was more difficult than in the simulator: In the flight test, pilots had to control the full motion of an aircraft along the tunnel in wind and turbulence, whereas in the simulator they controlled only the lateral motion of a simplified, linear aircraft model. In the simulator, pilots only experienced the consequences of their control actions on the aircraft maneuvering from the tunnel display. The aircraft rotation rates and accelerations were much higher than in the flight test, where pilots were reluctant to adopt a fierce, high-bandwidth control strategy. The fact that motion cues affect pilot behavior in flying the tunnel display has been reported in another study, where pilots rated the tunnel tracking task to be of higher workload when simulator motion was on than when it was off.[28] These findings altogether mean that one has to be careful in extrapolating measures of pilot performance and workload from a fixed-base flight simulator to real flight.

Second, whereas in the simulator the tunnel size could be decreased to 10 m, in the flight tests the tunnel size of 20 m was clearly too small for the most experienced pilot. Here a boundary has been exceeded where this pilot could not, or would not, perform any better. In any case, it is recommended not to make the tunnel too small. Rather, based on pilot comments, one could adopt an ILS-like funnellike geometry for the tunnel when on final approach.

Concluding, the flight test provides more, qualitative, evidence for Wilckens's[2] claim that there exists a boundary to tracking performance. Whether this is caused by the need for stability is unknown. Another possible cause is that pilots are likely to dampen their controls because of the (in their experience) excessive aircraft maneuvering that would be required for the smallest tunnels.

Conclusions

Pilot path-following performance with perspective flight-path displays is driven by the size of the virtual tunnel, and a tradeoff exists between pilot workload and the required tracking performance. A fixed-base flight simulator experiment, as well as a flight test, confirmed the theoretical findings. Both experiments showed that pilot performance increases for the smaller tunnels, at the cost of pilot workload. Through the use of pilot model identification, the effects of manipulating the tunnel size can be directly related to pilot/vehicle bandwidth and stability margins. The smallest tunnels reduce the stability margins considerably, and this should be prevented, not only from the perspective of pilot workload, but also for the benefit of safety. In critical tasks as landing an aircraft considerable margins should exist with respect to the stability of the pilot/aircraft control system. In comparison to the flight simulator experiment, the flight test showed that, for the smallest tunnels, pilots are reluctant to adopt a control strategy that leads to excessive maneuvering. Hence, experiments that address pilot workload and performance with a perspective flight-path display need to be conducted in a realistic task environment.

References

[1]Wilckens, V., "On the Dependence of Information Display Quality Requirements Upon Human Characteristics and 'Pilot/Automatics'-Relations," *Proceedings of the Seventh Annual Conference on Manual Control*, NASA SP-281, 1971, pp. 177–183.

[2]Wilckens, V., "Improvements in Pilot/Aircraft-Integration by Advanced Contact Analog Displays," *Proceedings of the Ninth Annual Conference on Manual Control*, MIT Press, Cambridge, MA, 1973, pp. 175–192.

[3]Grunwald, A. J., Robertson, J. B., and Hatfield, J. J., "Evaluation of a Computer-Generated Perspective Tunnel Display for Flight-Path Following," NASA TP-1736, 1980.

[4]Grunwald, A. J., "Tunnel Display for Four-Dimensional Fixed-Wing Aircraft Approaches," *Journal of Guidance and Control*, Vol. 7, No. 3, 1984, pp. 369–377.

[5]Roscoe, S. N., and Jensen, R. S., "Computer-Animated Predictive Displays for Microwave Landing Approaches," *IEEE Transactions on Systems, Man, and Cybernetics*, Vol. SMC-11, No. 11, 1981, pp. 760–765.

[6]Theunissen, E., "Integrated Design of a Man-Machine Interface for 4-D Navigation," Ph.D. Dissertation, Faculty of Electrical Engineering, Delft Univ. of Technology, Delft, The Netherlands, 1997.

[7]Mulder, M., "Cybernetics of Tunnel-in-the-Sky Displays," Ph.D. Dissertation, Faculty of Aerospace Engineering, Delft Univ. of Technology, Delft, The Netherlands, 1999.

[8]Sachs, G., "Perspective Predictor/Flight-Path Display with Minimum Pilot Compensation," *Journal of Guidance, Control, and Dynamics*, Vol. 23, No. 3, 2000, pp. 420–429.

[9]Parrish, R. V., Busquets, A. M., Williams, S. P., and Nold, D. E., "Spatial Awareness Comparisons Between Large-Screen, Integrated Pictorial Displays and Conventional EFIS Displays During Simulated Landing Approaches," NASA TP-3467, Oct. 1994.

[10]Regal, D., and Whittington, D., "Guidance Symbology for Curved Flight Paths," *Proceedings of the Eighth International Symposium on Aviation Psychology*, Ohio State Univ., Columbus, OH, 1995, pp. 74–79.

[11]Funabiki, K., "Tunnel-in-the-Sky Display Enhancing Autopilot Mode Awareness," *Conference Proceedings of the 1997 CEAS Free Flight Symposium*, NLR, Amsterdam, 1997, pp. 29.1–29.11.

[12]Theunissen, E., and Mulder, M., "Error-Neglecting Control with Perspective Flightpath Displays," *Proceedings of the Eighth International Symposium on Aviation Psychology*, Ohio State Univ., Columbus, OH, 1995, pp. 110–115.

[13]Theunissen, E., and Mulder, M., "Pilot-in-the-Loop Studies into Manual Control Strategies with Perspective Flightpath Displays," *Proceedings of the XIVth European Annual Conference on Human Decision Making and Manual Control*, Delft Univ. of Technology, Delft, The Netherlands, 1995, pp. 1.3.1–1.3.7.

[14]Theunissen, E., "Influence of Error Gain and Position Prediction on Tracking Performance and Control Activity with Perspective Flight Path Displays," *Air Traffic Control Quarterly*, Vol. 3, No. 2, 1995, pp. 95–116.

[15]Mulder, M., and Mulder, J. A., "Tunnel Size in a Tunnel-in-the-Sky Display: A Cybernetic Analysis," *Proceedings of the Seventh IFAC/IFIP/IFORS/IEA Symposium on Analysis, Design and Evaluation of Man-Machine Systems*, 1998, pp. 335–340.

[16]Mulder, M., Kraeger, A. M., and Soijer, M. W., "Delft Aerospace Tunnel-in-the-Sky Flight Tests," AIAA Paper 2002-4929, Aug. 2002.

[17]Grunwald, A. J., "Predictor Laws for Pictorial Flight Displays," *Journal of Guidance and Control*, Vol. 8, No. 5, 1985, pp. 545–552.

[18]Grunwald, A. J., "Improved Tunnel Display for Curved Trajectory Following: Control Considerations," *Journal of Guidance, Control, and Dynamics*, Vol. 19, No. 2, 1996, pp. 370–377.

[19]McRuer, D. T., and Jex, H. R., "A Review of Quasi-Linear Pilot Models," *IEEE Transactions on Human Factors in Electronics*, Vol. HFE-8, No. 3, 1967, pp. 231–249.

[20]Mulder, M., "An Information-Centered Analysis of the Tunnel-in-the-Sky Display, Part One: Straight Tunnel Trajectories," *International Journal of Aviation Psychology*, Vol. 13, No. 1, 2003, pp. 49–72.

[21]Mulder, M., "An Information-Centered Analysis of the Tunnel-in-the-Sky Display, Part Two: Curved Tunnel Trajectories," *International Journal of Aviation Psychology*, Vol. 13, No. 2, 2003, pp. 131–151.

[22]Gibson, J. J., *The Ecological Approach to Visual Perception*, Lawrence Erlbaum Associates, Hillsdale, NJ, 1986.

[23]Flach, J. M., Hagen, B. A., and Larish, J. F., "Active Regulation of Altitude as a Function of Optical Texture," *Perception and Psychophysics*, Vol. 51, No. 6, 1992, pp. 557–568.

[24]Larish, J. F., and Flach, J. M., "Sources of Optical Information Useful for Perception of Speed of Rectilinear Self-Motion," *Journal of Experimental Psychology: Human Perception and Performance*, Vol. 16, No. 2, 1990, pp. 295–302.

[25]McDonnel, J. D., "Pilot Rating Techniques for the Estimation and Evaluation of Handling Qualities," U.S. Air Force Flight Dynamics Lab., Technical Rept. AFFDL-TR-68-76, Wright–Patterson AFB, OH, 1968.

[26]Soijer, M. W., "Software-Enabled Modular Instrumentation Systems," Ph.D. Dissertation, Faculty of Aerospace Engineering, Delft Univ. of Technology, Delft, The Netherlands, 2003.

[27]Hart, S. G., and Staveland, L. E., "Development of NASA-TLX (Task Load Index): Results of Empirical and Theoretical Research," *Human Mental Workload*, edited by P. A. Hancock and N. Meshkati, Elsevier Science, North-Holland, Amsterdam, 1988, pp. 139–183.

[28]Mulder, M., Chiecchio, J., Pritchett, A. R., and van Paassen, M. M., "Testing Tunnel-in-the-Sky Displays and Flight Control Systems with and Without Flight Simulator Motion," *Proceedings of the 12th International Symposium on Aviation Psychology*, Wright State Univ., Dayton, OH, 2003, pp. 839–844.